Hindawi
Shock and Vibration
Volume 2021, Article ID 5592858, 9 pages
https://doi.org/10.1155/2021/5592858

Research Article

Random Dynamic Response Characteristics of Pipeline Subjected to Blasting Cylindrical SH Waves

Shiwei Lu,[1] **Heng Zhang**,[1] **and Ling Ji**[2]

[1]*School of Urban Construction, Yangtze University, Jingzhou 434023, China*
[2]*Faculty of Engineering, China University of Geosciences, Wuhan 430074, China*

Correspondence should be addressed to Heng Zhang; hengzhang@yangtzeu.edu.cn

Received 5 February 2021; Revised 10 May 2021; Accepted 8 July 2021; Published 19 July 2021

Academic Editor: Bangbiao Wu

It is essential to investigate the influence of blasting vibrations on pipelines, and the dynamic response is the crux in the safety issues. At present, the blasting seismic wave is usually regarded as a plane wave. However, there is little research about the dynamic response characteristics of underground structures subjected to nonplane waves. The analytical solution to dynamic stress concentration factor (DSCF) of pipelines subjected to cylindrical SH wave was derived. Besides, the randomness of the shear modulus of soil was considered, and the statistical analysis of DSCF was carried out by the Monte Carlo simulation method. Results show that the variability of the shear modulus of soil has a significant influence on the probability distribution of DSCF. The larger the variation coefficient of the shear modulus is, the more obvious the skewness of DSCF is. The influence of low-frequency wave on pipeline increases with the reducing normalized distance r^*, while the influence of high-frequency wave reduces and the variation amplitude of DSCF increases. Compared with the DSCF of pipe subjected to a plane wave, a lower dominant frequency or larger normalized distance for the cylindrical SH wave will generate a more similar statistical characteristic of DSCF.

1. Introduction

With the rapid development of transportation construction, the drilling and blasting method has been widely used in the excavation of underground space due to its efficiency and economy. However, blasting seismic waves induced by the structures excavation will undermine the safety of nearby pipelines which are important channels for energy transmission and even cause serious economic losses and successive disasters.

A large number of research studies have been implemented to study the dynamic response characteristics of underground structures subjected to blasting seismic waves. Pao and Mow [1] investigated the dynamic stress concentration factors (DSCFs) of a cavity in an unbounded elastic space under the incident plane P, SH, and SV waves. Lee and Trifunac [2–4] studied the dynamic response of tunnels and cavities induced by plane P, SH, and SV waves. Thambirajah et al. [5] considered the effect of DSCF and studied the scattering of SH waves by two caverns. Liu and Wang [6] revealed the dynamic response law of cavities subjected to plane waves. Wang et al. [7] used the wave function expansion method to give an analytical solution to the dynamic response of a deep-buried soft rock circular tunnel under the incident plane SH wave. Fu et al. [8] studied the interaction between the soil and the tunnel when the blasting plane SH wave was considered. Yi et al. [9] proposed an analytical solution to the dynamic response of a circular tunnel when the imperfect contact exists between surrounding rock and lining subjected to incident plane P waves. Liu et al. [10] used the complex functions and multilevel coordinate method to analyze the influence of P wave on pipelines in saturated soil. He et al. [11] studied the scattering of plane SH waves by underground caverns with arbitrary cross-sectional shapes. Zhang et al. [12] derived the analytical solution to the dynamic responses of deep-water foundation sites when both incident plane P and SV waves were considered. Liang et al. [13] studied the diffraction of plane SH waves by a

semicircular cavity in half-space by using the wave function expansion method. Xu et al. [14] deduced a series solution of dynamic stress for a circular lining tunnel subjected to incident plane P waves in an elastic half-space. Xu [15] derived the blasting safety criterion of an unlined circular tunnel subjected to plane P waves. Qi et al. [16, 17] carried out the dynamic analysis for circular inclusions near interface impacted by SH waves using the complex method and Green's function method. Fan et al. [18] predicted the dynamic response of a circular lined tunnel with an imperfect interface to plane SV waves based on the wave function expansion method and the linear spring model. Lu et al. [19] studied the dynamic stress concentration and vibration velocity scaling factors of an unlined circular tunnel subjected to a triangular P wave. Xia et al. [20] calculated the vibration response of buried flexible HDPE pipes under impact loads based on the Winkler model and the Timoshenko beam theory. Recently, Jiang et al. [21–23] studied the dynamic failure behavior of buried cast iron gas pipeline subjected to blasting vibration. In order to simplify the analysis, most of these studies approximately regard blasting seismic waves as plane waves. However, the assumption is not reliable when the explosion source is close to the underground structure because the curvature of incident blasting waves cannot be ignored. Although some research studies about cylindrical waves have been carried out, the random dynamic response of underground structures under cylindrical waves is still rare in literature [24–26].

At present, He and Liang [27] used the Monte Carlo simulation method to study the influence of the shape variability of the outer wall on the peak value of DSCF around the inner wall. However, due to the effects of multiple factors, such as sedimentation, weathering, chemical action, transportation processes, and different loading history, the physical and mechanical properties of rock and soil vary spatially. Therefore, it is more suitable to study the DSCF of pipelines under cylindrical SH waves when the shear modulus of soil is considered as random parameter.

2. Random Dynamic Responses of Pipeline Subjected to Cylindrical SH Waves

2.1. Simplified Model. A linear wave source is assumed to locate at O_1, and the axis of a circular pipe whose inner and outer radius are a and b, respectively, coincides with O_2. The distance between O_1 and O_2 is r_0, and the coordinate systems $O_1x_1y_1$ and $O_2x_2y_2$ are established on O_1 and O_2, respectively, as shown in Figure 1. P is an arbitrary point in the soil, and the distances away from O_1 and O_2 are r_1 and r_2, respectively. The displacement function of the cylindrical SH wave generated at O_1 can be expressed in the following form [28, 29]:

$$W^{(i)} = H_0^{(1)}(\beta_1 r_1)\exp(-i\omega t), \tag{1}$$

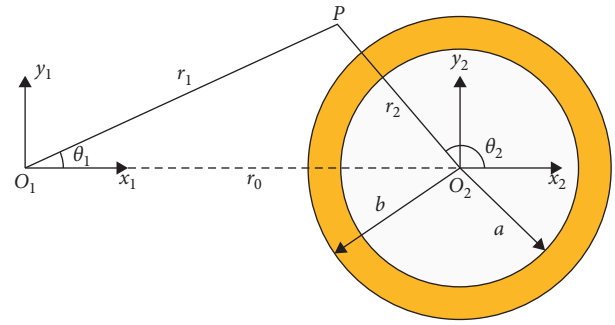

Figure 1: Incident cylindrical SH wave.

where $H_0^{(1)}$ is the 0th-order Hankel function, i is the imaginary unit, β_1 is the wave number of SH wave in the soil, and $\beta_1 = \omega/c_{s1}$, in which ω is the frequency of the incident wave and $c_{s1} = \sqrt{G/\rho}$ is the speed of SH wave in the soil. ρ is the density of the soil. The shear modulus G of the soil is considered as a random parameter, which can be described as

$$G(\xi) = \overline{G}(1 + \alpha\xi), \tag{2}$$

where $\overline{G}$ is the mean value of the shear modulus of soil and ξ is a random variable with standard normal distribution $N(0,1)$. As a result, the shear modulus of the soil G and the SH wave-number β_1 will be a function of the random variable ξ. Then, the coefficient of variation (Cov) of the shear modulus δ_G of the soil can be calculated as

$$\delta_G = \frac{\sqrt{\mathbf{D}[G(\xi)]}}{\mathbf{E}[G(\xi)]} = \alpha. \tag{3}$$

Generally, when a cylindrical SH wave reaches the pipe, it will generate a reflected SH wave ($W^{(r)}$) propagating outward in the soil and a refracted SH wave ($W^{(f)}$) propagating outward and inward in the pipe. Their displacement can be expressed as follows:

$$\begin{cases} W^{(r)} = \sum_{n=0}^{\infty} H_n^{(1)}[\beta_1(\xi)r_2][B_n\cos n\theta_2 + E_n\sin n\theta_2]\exp(-i\omega t), \\ W^{(f)} = \sum_{n=0}^{\infty} H_n^{(1)}(\beta_2 r_2)[C_n\cos n\theta_2 + F_n\sin n\theta_2]\exp(-i\omega t) \\ \quad + \sum_{n=0}^{\infty} H_n^{(2)}(\beta_2 r_2)[D_n\cos n\theta_2 + G_n\sin n\theta_2]\exp(-i\omega t), \end{cases} \tag{4}$$

where $\beta_2 = \omega/c_{s2}$ is the wave number of SH waves in the pipe and $c_{s2} = \sqrt{G_2/\rho_2}$ is the speed of SH wave in the pipe, in which G_2 is the shear modulus of the pipe and ρ_2 is the density of the pipe.

In order to obtain the displacement function of the incident wave, the reflected wave, and the refracted wave, the incident wave potential function in the $O_1x_1y_1$ coordinate system must be converted to the expression form in the $O_2x_2y_2$ coordinate system. The conversion formula is expressed as follows [30, 31]:

$$H_n^{(1)}[\beta_1(\xi)r_1]\cos n\theta_1 = \sum_{m=-\infty}^{\infty}(-1)^m H_m^{(1)}[\beta_1(\xi)r_0]J_{m+n}[\beta_1(\xi)r_2]\cos(m+n)\theta_2, \quad (5)$$

where $H_n^{(1)}$ is the nth-order Hankel function and J_n is the nth-order Bessel function.

Substituting equation (5) into equation (1), we can express the displacement function of the cylindrical SH wave as follows:

$$W^{(i)} = \sum_{n=0}^{\infty} A_{0n}J_n[\beta_1(\xi)r_2]\cos n\theta_2 \exp(-i\omega t), \quad (6)$$

where $A_{0n} = (-1)^n \epsilon_n H_n^{(1)}[\beta_1(\xi)r_0]$; if $n = 0$, $\epsilon_0 = 1$; when $n > 0$, $\epsilon_0 = 2$.

2.2. Boundary Conditions. Let $W_1 = W^{(i)} + W^{(r)}$ and $W_2 = W^{(f)}$; considering the interface between the pipe and the soil as an ideal contact interface, the boundary conditions can be expressed as follows:

$$\begin{cases} \tau_{rz1} = \tau_{rz2},\ W_1 = W_2, & \text{if } r_2 = b, \\ \tau_{rz2} = 0, & \text{if } r_2 = a. \end{cases} \quad (7)$$

The relationship between the displacement and the stress of a cylindrical SH wave can be expressed as follows:

$$\tau_{rz} = \frac{\mu}{\partial r}\frac{\partial W}{\partial r}, \qquad \tau_{\theta z} = \frac{\mu}{r}\cdot\frac{\partial W}{\partial \theta}. \quad (8)$$

According to equations (5) and (8), the value of B_n, C_n, D_n, E_n, F_n, and G_n can be obtained.

2.3. Solution of Random DSCF Based on the Monte Carlo Simulation Method. In order to obtain general results, the dimensionless parameters of DSCF and normalized distance r^* are defined as follows:

$$\mathrm{DSCF} = \max\left|\frac{\tau_{\theta z2}}{\tau_{rz1}^{(i)}}\right|, \quad (9)$$

$$r^* = \frac{r_0}{b}, \quad (10)$$

where $\tau_{rz1}^{(i)} = -\mu_1\beta_1(\xi)H_1^{(1)}[\beta_1(\xi)r_1]$.

When the randomness of structural parameters is considered, the dynamic response of the structure will also be random. In order to obtain the random response of the structure, a series of various strategies such as the Monte Carlo simulation method [32], stochastic finite element method [33], and the probability density evolution method [34] are proposed. The Monte Carlo simulation method has a high calculation accuracy in solving complex functions. Besides, the calculation accuracy is not affected by the variability of random parameters. Therefore, it is widely used in theoretical research studies. Owing to the given explicit formula of DSCF, the Monte Carlo simulation method is adopted to obtain the statistical results of DSCF. The main steps are as follows:

Step 1. Use equation (2) to describe the randomness of the shear modulus of the soil and generate a sufficient number of samples ξ which obeys the standard normal distribution

Step 2. According to the derivation process of DSCF, substitute each sample into the expression of the shear modulus of soil and obtain the corresponding result of DSCF

Step 3. Perform statistical analysis on the samples of DSCF obtained in Step 2

3. Engineering Background

The underground passage of Baotong Temple passes through the concrete sewage pipe at a short distance and is excavated by drilling and blasting. The top of the passage is only 0.69 m away from the sewage pipe. The density and shear modulus of the pipeline are 2400 kg/m^3 and 12.61 GPa, respectively. The inner radius a and the outer radius b are 400 mm and 465 mm, respectively. The density of the surrounding soil is 1980 kg/m^3, and the average shear modulus of the soil $\overline{G}$ is 150 MPa. According to the construction information, the dominant frequency of blasting seismic waves is below 200 Hz. Consequently, the dominant frequency f and r_0 are considered as 10~200 Hz and $2b$~$10b$, respectively. δ_G is selected as 0.1 and 0.2, respectively, in the following analysis.

4. Results and Discussion

4.1. Convergence Analysis. The Monte Carlo simulation method is employed to obtain the statistical results of the DSCF. First, a certain number of samples which obey the standard normal distribution are generated, then the random shear modulus is expressed using equation (2), and finally the sample values of the DSCF are calculated through equations (4)–(9).

Before the implementation of the Monte Carlo simulation progress, it is necessary to study the influence of the number of the samples on the convergence of the solution. Figure 2 exhibits the first four statistic moments (mean, standard deviation, skewness, and kurtosis) of DSCF generated by the Monte Carlo simulation method with the number of the samples increasing from 1×10^3 to 5×10^5 when the four dominant frequencies are 10 Hz, 50 Hz, 100 Hz, and 200 Hz, respectively. It is found that in the aspects of mean and standard deviation, only a small number of samples is needed to obtain stable results regardless of f. However, in the aspects of skewness and kurtosis, a large number of samples are required. It indicates that a sufficient large number of samples are necessary to obtain stable high-order statistical moments of DSCF to ensure the convergence. For example, the calculation results of the first four

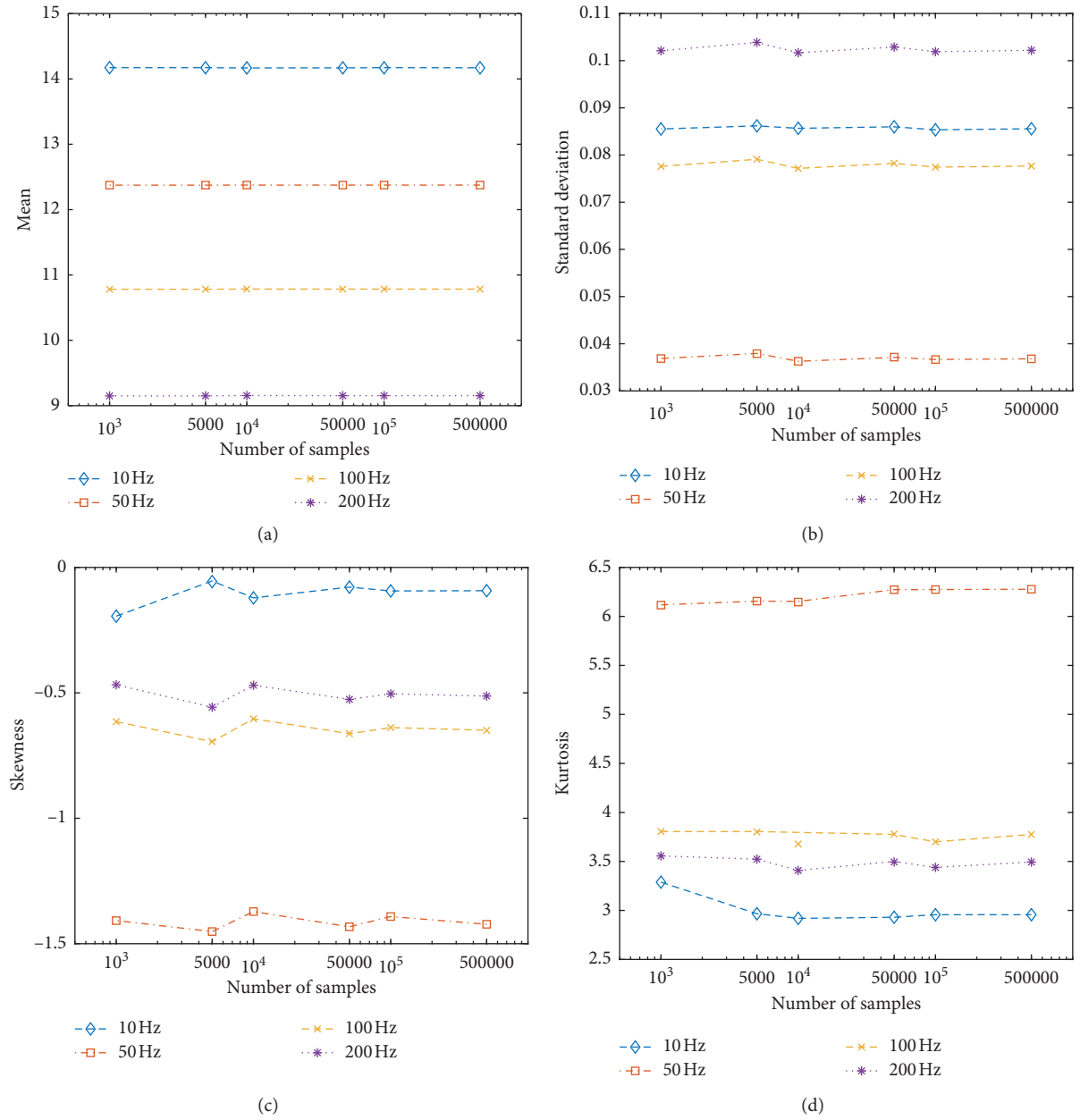

Figure 2: First four statistic moments of DSCF obtained with different numbers of samples: (a) mean; (b) standard deviation; (c) skewness; (d) kurtosis.

statistic moments tend to be stable when more than 100,000 samples are selected, and thus 100,000 samples should be used in the subsequent analysis.

Figure 3 shows the mean and standard deviation of the DSCF when different values of r^* are considered. It is observed from Figure 3 that when δ_G is equal to 0.1 and 0.2, the mean of the DSCF decreases significantly when the dominant frequency increases. When the dominant frequency is equal to 50 Hz, 100 Hz, and 200 Hz, the standard deviation of DSCF decreases with the increasing r^*, especially when $2 \le r^* \le 5$. However, the standard deviation of DSCF is almost unchanged when $f = 10$ Hz.

4.2. Analysis of the Pipeline Dynamic Response Characteristics. Figures 4 and 5 show the probability density function (PDF) curve and cumulative distribution function (CDF) curve of DSCF when $\delta_G = 0.1$ and 0.2, respectively. DSCF of the pipeline under the plane wave is also provided for comparison.

It can be seen from Figure 4 that when δ_G is small (i.e., $\delta_G = 0.1$), the PDF of DSCF approximately obeys the Gaussian distribution when $f = 10$ Hz. With the increase in r^*, the PDF curve integrally shifts to the left, which suggests that the mean of the DSCF reduces. However, the mean of DSCF increases with the increase in r^* when f is equal to

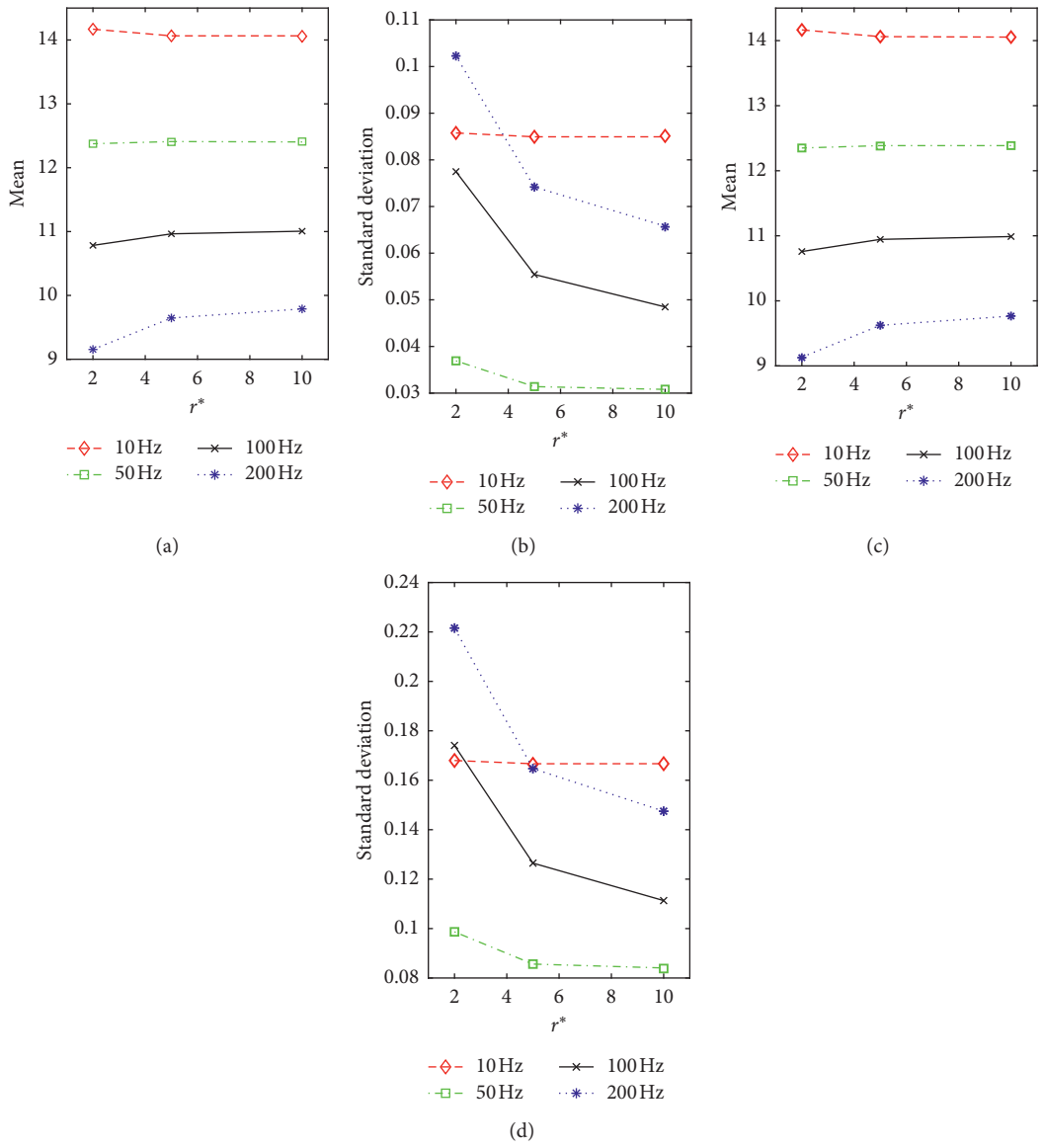

FIGURE 3: Mean and standard deviation of DSCF for different values of r^*: (a) mean ($\delta_G = 0.1$); (b) standard deviation ($\delta_G = 0.1$); (c) mean ($\delta_G = 0.2$); (d) standard deviation ($\delta_G = 0.2$).

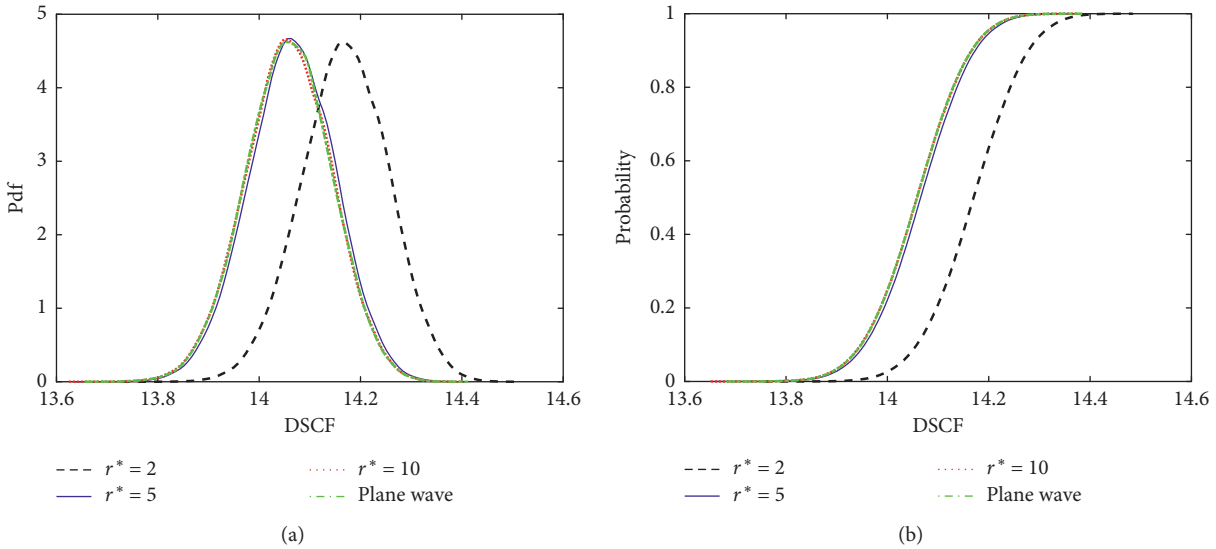

FIGURE 4: Continued.

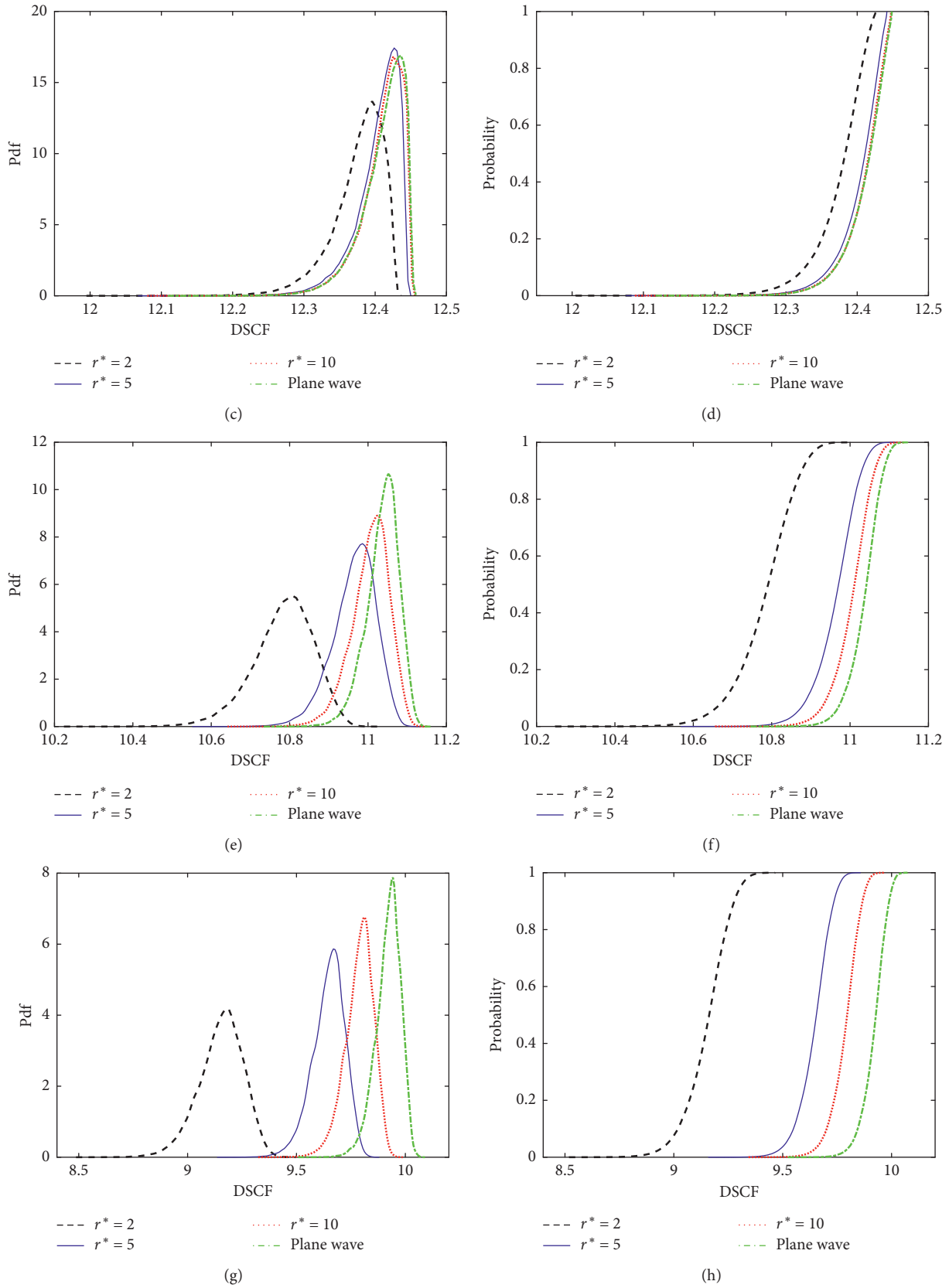

FIGURE 4: PDF curves (left) and CDF curves (right) of DSCF when $\delta_G = 0.1$: (a) PDF $f = 10$ Hz; (b) CDF $f = 10$ Hz; (c) PDF $f = 50$ Hz; (d) CDF $f = 50$ Hz; (e) PDF $f = 100$ Hz; (f) CDF $f = 100$ Hz; (g) PDF $f = 200$ Hz; (h) CDF $f = 200$ Hz.

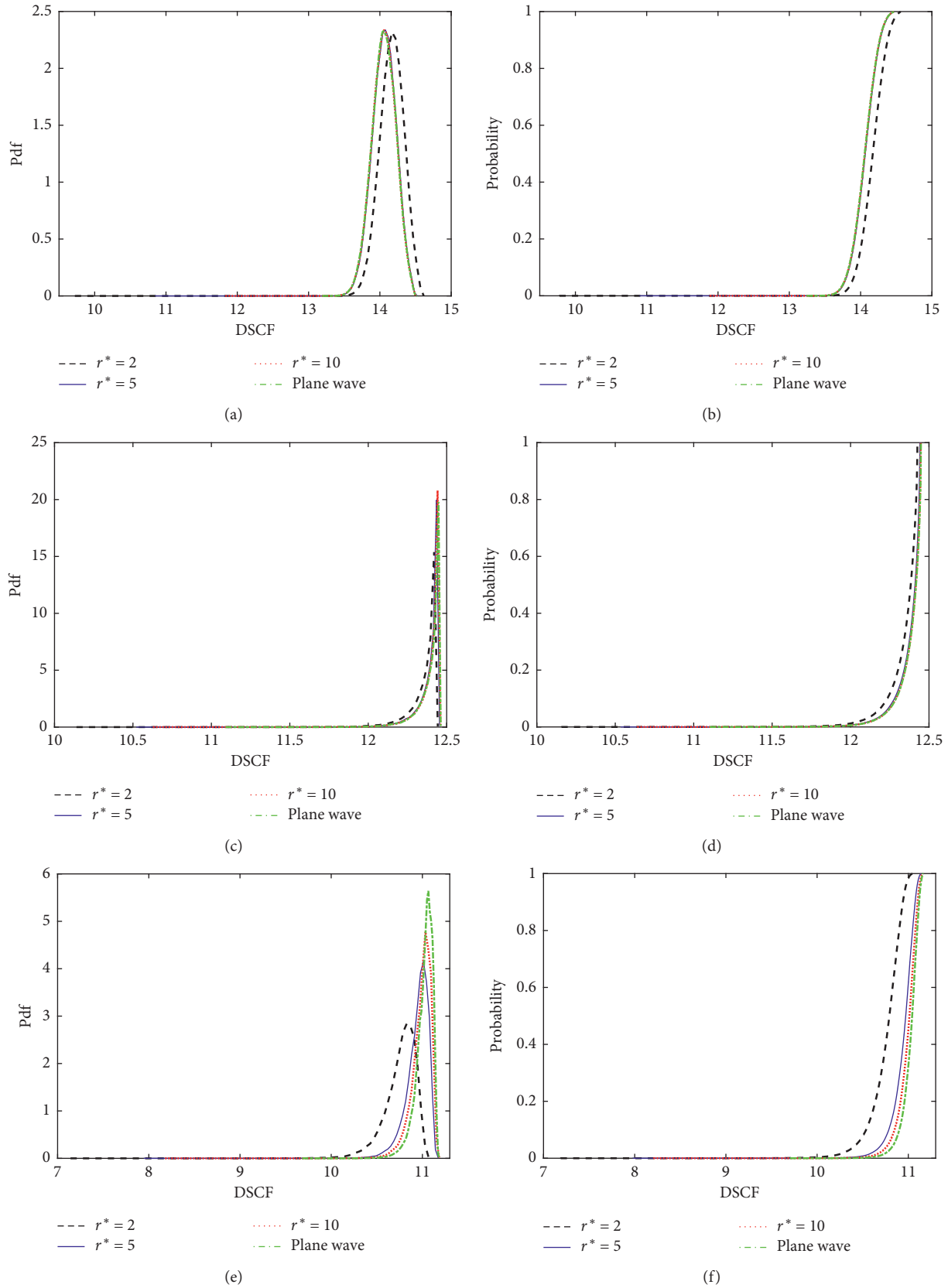

Figure 5: Continued.

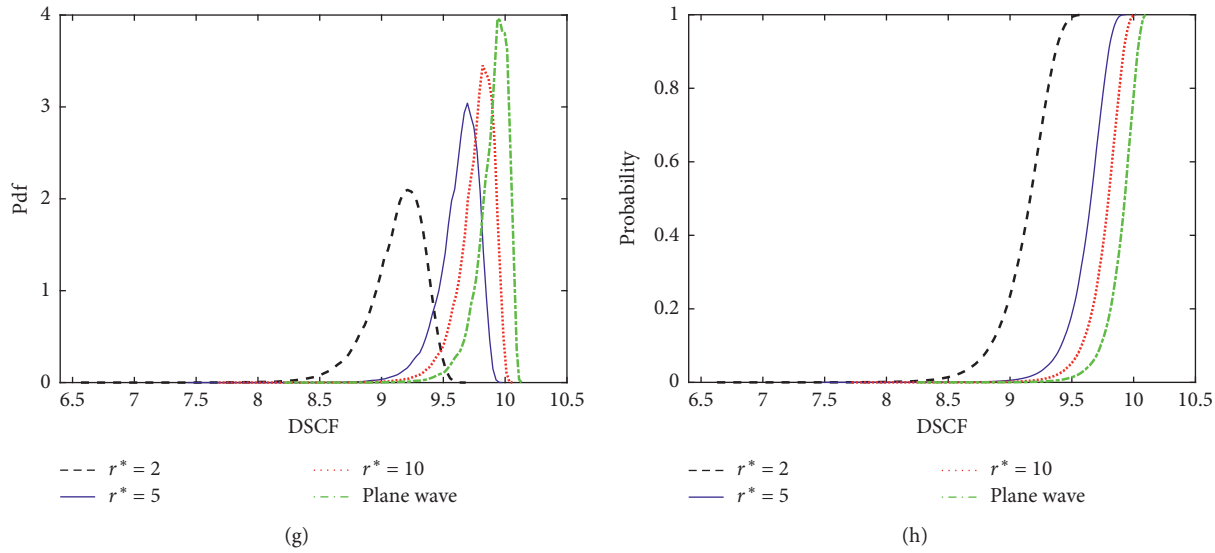

Figure 5: PDF curves (left) and CDF curves (right) of DSCF when $\delta_G = 0.2$: (a) PDF $f = 10$ Hz; (b) CDF $f = 10$ Hz; (c) PDF $f = 50$ Hz; (d) CDF $f = 50$ Hz; (e) PDF $f = 100$ Hz; (f) CDF $f = 100$ Hz; (g) PDF $f = 200$ Hz; (h) CDF $f = 200$ Hz.

50 Hz, 100 Hz, and 200 Hz. The PDF curve when $f = 50$ Hz is obviously different from that of other cases. When the dominant frequency is relatively small (10 Hz or 50 Hz), the PDF and CDF of DSCF generated by the cylindrical SH wave are very similar to the results of the plane wave. As the dominant frequency increases, the distinctions between the cylindrical SH wave and plane wave will appear; however, the PDF and CDF of DSCF are getting close to the results of the plane wave as r^* increases.

It is found from Figure 5 that the variation of the mean of DSCF with r^* is similar when δ_G is equal to 0.1 and 0.2, respectively. However, all the PDF curves of DSCF become leftward, and they do not obey the normal distribution any more, especially in the case of $f = 50$ Hz. A comparison between Figures 4 and 5 shows that the larger δ_G is, the more obvious the skewness of PDF is, which indicates that the relationship of DSCF and shear modulus of soil is significantly nonlinear. Compared with the DSCF under the plane wave, it has a same trend as $\delta_G = 0.1$; a lower dominant frequency or larger normalized distance under the cylindrical SH wave will obtain a closer result.

5. Conclusions

(1) The shear modulus of soil is defined as a random parameter, and the analytical expression of the maximum DSCF of pipe subjected to an incident cylindrical SH wave is established based on the Fourier–Bessel expansion and the Monte Carlo simulation method.

(2) When the dominant frequency is 10 Hz, the mean and median of DSCF decrease as the normalized distance increases. However, this is contrary to those when the frequency of incident wave is 50 Hz, 100 Hz, and 200 Hz, which indicates that when the normalized distance is small, the lower-frequency wave has a greater impact on the pipeline than the higher-frequency wave.

(3) With the increase in normalized distance, the PDF of DSCF gradually becomes narrow, indicating that the variability of DSCF decreases with the increase in normalized distance.

(4) Compared with the DSCF of pipe subjected to a plane wave, a lower dominant frequency or larger normalized distance for the cylindrical SH wave will generate much closer PDF and CDF of DSCF.

Data Availability

The data used to support the findings of this study are included within the article.

Conflicts of Interest

The authors declare that they have no conflicts of interest.

Acknowledgments

The study was sponsored by Hubei Provincial Natural Science Foundation (Grant no. 2019CFB224), Hubei Provincial Department of Education (Grant no. Q20191308), and Open Research Fund of Hubei Key Laboratory of Blasting Engineering (Grant no. HKLBEF202011).

References

[1] Y. H. Pao and C. C. Mow, *Diffraction of Elastic Waves and Dynamic Stress Concentrations*, Crane Russak, New York, NY, USA, 1973.

[2] V. W. Lee and M. D. Trifunac, "Response of tunnels to incident SH-waves," *Journal of the Engineering Mechanics Division*, vol. 105, no. 4, pp. 643–659, 1979.

[3] V. W. Lee and J. Karl, "Diffraction of SV waves by underground, circular, cylindrical cavities," *Soil Dynamics and Earthquake Engineering*, vol. 11, no. 8, pp. 445–456, 1992.

[4] V. W. Lee and J. Karl, "On deformation near a circular underground cavity subjected to incident plane P waves," *European Journal of Earthquake Engineering*, vol. 6, no. 1, pp. 29–35, 1993.

[5] B. Thambirajah, P. T. David, G. K. Chan et al., "Dynamic response of twin circular tunnels due to incident SH-waves," *Earthquake Engineering & Structural Dynamics*, vol. 12, no. 2, pp. 181–201, 1984.

[6] Z. X. Liu and D. Wang, "FMM-MFS solution to two-dimensional scattering of elastic waves," *Journal of Vibration and Shock*, vol. 34, no. 5, pp. 102–109, 2015.

[7] S. S. Wang, B Gao, Y. S. Shen et al., "Study on the mechanism of resistance and damping technology of deep soft rock tunnels subjected to incident plane SH waves," *China Civil Engineering Journal*, vol. 47, no. S1, pp. 280–286, 2014.

[8] J. Fu, J. W. Liang, and J. J. Du, "Analytical solution of dynamic soil-tunnel interaction for incident plane SH wave," *Chinese Journal of Geotechnical Engineering*, vol. 38, no. 4, pp. 588–598, 2016.

[9] C. P. Yi, W. B. Lu, P. Zhang et al., "Effect of imperfect interface on the dynamic response of a circular lined tunnel impacted by plane P-waves," *Tunnelling and Underground Space Technology incorporating Trenchless Technology Research*, vol. 51, pp. 68–74, 2016.

[10] Y. P. Liu, L. Qiao, and B. Xu, "Dynamic response of liquid-filled pipe embedded in saturated soil due to P waves," *Rock and Soil Mechanics*, vol. 34, no. 11, pp. 3151–3158, 2013.

[11] Y. He, J. W. Liang, and Y. X. Lin, "Effect of cross-section-shape randomness of underground cavity on scattering of plane SH waves," *Earthquake Engineering and Engineering Vibration*, vol. 34, no. 1, pp. 1–7, 2014.

[12] K. Zhang, L. H. Wei, and C. G. Zhao, "Dynamic responses of an underwater site subjected to plane P-or SV-wave incidence," *Chinese Journal of Geotechnical Engineering*, vol. 40, no. 6, pp. 1066–1074, 2018.

[13] J. W. Liang, H. Luo, and V. W. Lee, "Diffraction of plane SH waves by a semi-circular cavity in half-space," *Earthquake Science*, vol. 23, no. 1, pp. 5–12, 2010.

[14] H. Xu, T. Li, J. Xu, and Y. Wang, "Dynamic response of underground circular lining tunnels subjected to incident P waves," *Mathematical Problems in Engineering*, vol. 2014, Article ID 297424, 11 pages, 2014.

[15] T. Xu, "Blasting vibration safety criterion of surrounding rock of a circular tunnel," *Geotechnical & Geological Engineering*, vol. 37, no. 4, pp. 3077–3084, 2019.

[16] H. Qi, J. Yang, and Y. Shi, "Scattering of sh-wave by cylindrical inclusion near interface in Bi-material half-space," *Journal of Mechanics*, vol. 27, no. 1, pp. 37–45, 2011.

[17] H. Qi, J. Yang, Y. Shi, and J. Y. Tian, "Dynamic analysis for circular inclusion near interfacial crack impacted by SH-wave in half space," *Journal of Mechanics*, vol. 28, no. 1, pp. 143–151, 2012.

[18] Z. Fan, J. Zhang, and H. Xu, "Theoretical study of the dynamic response of a circular lined tunnel with an imperfect interface subjected to incident SV-waves," *Computers and Geotechnics*, vol. 110, pp. 308–318, 2019.

[19] S. W. Lu, C. B. Zhou, Z. Zhang et al., "Theoretical study on dynamic responses of an unlined circular tunnel subjected to blasting P-waves," *Journal of Mechanics*, vol. 37, no. 4, pp. 242–252, 2021.

[20] Y. Xia, N. Jiang, C. Zhou, X. Meng, X. Luo, and T. Wu, "Theoretical solution of the vibration response of the buried flexible HDPE pipe under impact load induced by rock blasting," *Soil Dynamics and Earthquake Engineering*, vol. 146, Article ID 106743, 2021.

[21] B. Zhu, N. Jiang, C. Zhou, X. Luo, Y. Yao, and T. Wu, "Dynamic failure behavior of buried cast iron gas pipeline with local external corrosion subjected to blasting vibration," *Journal of Natural Gas Science and Engineering*, vol. 88, Article ID 103803, 2021.

[22] N. Jiang, B. Zhu, X. He, C. Zhou, X. Luo, and T. Wu, "Safety assessment of buried pressurized gas pipelines subject to blasting vibrations induced by metro foundation pit excavation," *Tunnelling and Underground Space Technology*, vol. 102, Article ID 103448, 2020.

[23] Q. C. Tang, N. Jiang, Y. K. Yao, C. B. Zhou, and T. Y. Wu, "Experimental investigation on response characteristics of buried pipelines under surface explosion load," *International Journal of Pressure Vessels and Piping*, vol. 183, Article ID 104101, 2020.

[24] J. W. Liang, M. Ding, and J. J. Du, "Diffraction of cylindrical SH waves around circular lined cavity: analytical solution," *Earthquake Engineering and Engineering Vibration*, no. 1, pp. 1–7, 2013.

[25] S. B. Chai, J. H. Zhao, and H. Wang, "UDEC simulation on cylindrical wave propagation through jointed rock masses," *Chinese Journal of Rock Mechanics and Engineering*, vol. 38, no. S1, pp. 2848–2856, 2019.

[26] S. W. Lu, C. B. Zhou, Z. Zhang et al., "Particle velocity response of surrounding rock of a circular tunnel subjected to cylindrical P-waves," *Tunnelling and Underground Space Technology*, vol. 83, pp. 393–400, 2019.

[27] Y. He and J. W. Liang, "Effect of outer-wall shape variation of underground lined cavity on inner-wall dynamic stress concentration factors peak values," *Chinese Journal of Rock Mechanics and Engineering*, vol. 34, no. S1, pp. 3160–3168, 2015.

[28] M. Abramowitz and I. A. Stegun, *Handbook of Mathematical Functions: With Formulas, Graphs, and Mathematical Tables*, Dover Publications Inc., NY, USA, 1964.

[29] X. L. Chen and M. J. Wen, "Dynamic characteristics of a cylindrical tunnel considering interaction between saturated soil and lining," *Chinese Journal of Applied Mechanics*, vol. 30, no. 4, pp. 557–562, 2013.

[30] C. P. Yi, P. Zhang, D. Johansson et al., "Dynamic response of a circular lined tunnel with an imperfect interface subjected to cylindrical P-waves," *Computers and Geotechnics*, vol. 55, pp. 165–171, 2014.

[31] S. W. Lu, C. B. Zhou, Z. Zhang et al., "Dynamic stress concentration of surrounding rock of a circular tunnel subjected to blasting cylindrical P-waves," *Geotechnical & Geological Engineering*, vol. 37, pp. 2363–2371, 2019.

[32] H. Niederreiter and J. Spanier, *Monte Carlo and Quasi-Monte Carlo Methods*, Springer, Berlin, Germany, 2000.

[33] M. Kleiber and T. D. Hien, *The Stochastic Finite Element Method*, John Wiley, Chichester, England, 1992.

[34] J. Li and J. B. Chen, "The probability density evolution method for analysis of dynamic nonlinear response of stochastic structures," *Chinese Journal of Applied Mechanics*, vol. 35, no. 6, pp. 716–722, 2003.